Structural Eng. / Earthquake Eng. Vol. 6. No. 1, 49s-57s. April 1989
Japan Society of Civil Engineers (Proc. of JSCE No. 404 / I-11)

PLANAR BUCKLING AND POST-BUCKLING BEHAVIORS OF RINGS AND ARCHES SUBJECT TO DISPLACEMENT DEPENDENT LOADS

By Akio HASEGAWA, Toru MATSUNO** and Fumio NISHINO****

The tangent stiffness equation for a planar straight beam to reflect the displacement dependency of loading is derived. The load stiffness matrices for water pressure and the center directed uniform distributive loading for circular members are obtained explicitly. Using the stiffness equation derived, planar buckling and post-buckling of elastic rings and arches subject to a variety of loading patterns have been examined. It is found from the computations that the displacement dependency of loadings significantly affects not only the buckling strength, but also, even more, the post buckling finite displacement behavior of the structures.

Keywords: buckling, post-buckling, ring, arch, displacement dependent load, FEM

1. INTRODUCTION

A variety of patterns can exist in displacement dependent loadings applicable for planar circular members such as gravity loads and water pressure. Displacement dependency definitely influences the buckling and post-buckling behavior of those structures, and a number of studies have been reported of this subject, either through a rather classical analytical[1)~6)] or a more advanced computational way[7)~9)]. However, those available seem to be rather vague in the treatments of loading and boundary conditions particularly in the classical analytical approach or to be complicated in the computational FEM approach. Recently, the authors have presented the analysis scheme for the elastic instability and nonlinear behavior of thin-walled members under non-conservative forces, and have demonstrated the interesting features of the follower forces and wind forces[10)]. The present paper, based on the same concept as Ref. 10), aims to present the FEM nonlinear analysis, focusing on the characteristics of the buckling and post-buckling behavior of rings and arches subjected to a wide pattern of displacement dependent loadings.

The present FEM analysis is based on the assembly of the well-known planar straight beam element, but newly develops the so-called load matrices which make it possible to investigate the influences of the change of the direction for a variety of loadings. The tangent stiffness equation of planar beams is derived using the virtual work equation of linearized finite displacements, incorporating the effects of the displacement dependency of the loads.

Based on the stiffness equation derived, firstly, the buckling analysis is made for a variety of loadings, and the results are compared with the rather classical existing solutions, if any. Secondly, the

* Member of JSCE, Dr. Eng., Professor, Department of Civil Engineering, Univ. of Tokyo (Bunkyo-ku, Tokyo).
** Member of JSCE, Mr. Eng., Ohbayashi-Gumi Co. Ltd., formerly Graduate Student, Department of Civil Engineering, Univ. of Tokyo (Bunkyo-ku, Tokyo).
*** Member of JSCE, Ph. D., Professor, Department of Civil Engineering, Univ. of Tokyo (Bunkyo-ku, Tokyo).

post-buckling elastic finite displacement behavior is traced using a non-iterative nonlinear updated Lagrangian formulation which has been proposed and proved reliable in Ref. 11). A special attention is paid on how the displacement dependency influences the post-buckling behavior of arches.

2. DISPLACEMENT DEPENDENT LOADING PATTERNS

Fig. 1 shows the five loading patterns to be investigated in this study, some of which have existing results, and the others are for the interest of comparison. The followings are brief explanations of the loading patterns to be examined.

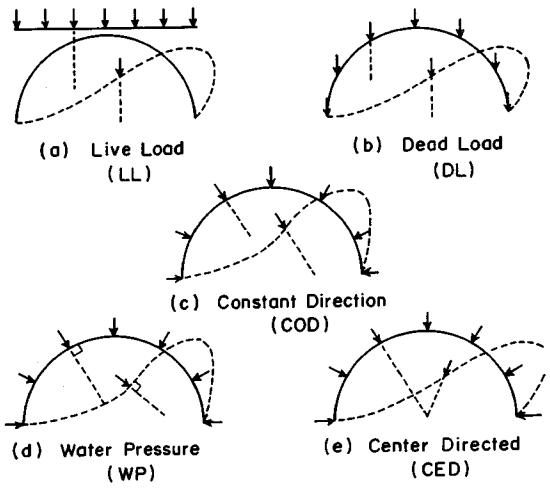

Fig. 1 Loading Pattern.

(a) Live Loading (LL) : Distributive loading is applied vertically and uniformly along the horizontal axis at the initial stage and the direction of load does not change during deformation. This represents the live load pattern in actual situation.

(b) Dead Loading (DL) : The same as the previous live loading except that the load is applied uniformly along the circular beam axis. It represents the dead load pattern in actual circumstances.

(c) Constant Direction Loading (COD) : Uniform distributive load along the beam axis is toward the centre of the circular arch at the initial stage, but the direction of load does not change, being away from the centre during deformation. This pattern is rather artificial.

(d) Water Pressure (WP) : Uniform distributive load along the beam axis is applied always prependicular to the beam axis both at the initial stage and during deformation. This pattern is well-known as water pressure.

(e) Center Directed Loading (CED) : Uniform distributive load along the beam axis is always toward the center of the circular arch both at the initial stage and during deformation. This may represent a kind of cable supported structures.

Among the five patterns described above, the direction of load does not change anyway during deformation for (a), (b) and (c) but the initial conditions differ each other. While, the initial conditions are exactly the same for (c), (d) and (e), but the direction of load differs during deformation. Among them, water pressure (d) is considered as non-conservative forces, while the others are conservative.

3. EXISTING RESULTS FOR BUCKLING STRENGTH

There exist a number of existing solutions[2)~6)] for the buckling strength of rings and arches. As for rings, the solutions have been obtained for (c), (d) and (e) according to the above classification, in all of which the load is toward the center of ring at the initial stage. In the case both of hinged and fixed circular arches, there have been two solutions, one for (c) and the other being not clearly specified. Those existing solutions have been given by the following buckling formula as

$$q_{cr}=k\frac{EI}{R^3} \qquad (1)$$

where EI and R are flexural rigidity and the radius of circular beam, respectively, and k is buckling coefficient depending on boundary and loading conditions. The existing solutions mentioned above were obtained semi-analytically under some constraints before the era of computers, and the process of derivation as well as the subsequent proof were ambiguous and somewhat unreliable, being subject to reexamination.

4. DERIVATION OF TANGENT STIFFNESS EQUATION

Based on the virtual work equation of linearized finite displacements[12] for a planar beam, the tangent stiffness equation is derived incorporating the influences of the change of direction of loads such as water pressure (d) and center directed loading (e).

Introducing the right hand Cartesian coordinates (x_i) or (x, y, z) with their desplacement components (u_i) or (u, v, w), the virtual work equation for the finite displacement theory of a general continuum with volume V and surface S is expressed as

$$\int_v [\overline{\sigma}_{ij}\delta\overline{e}_{ij}]\,dV-\int_v [\overline{p}_i\delta\overline{u}_i]\,dV-\int_s [\overline{T}_i\delta\overline{u}_i]\,dS=0 \cdots\cdots (2)$$

where $\overline{\sigma}_{ij}$ is the second Piola-Kirchhoff stress tensor, $\overline{e}_{ij}$ is Green's strain tensor, and $\overline{p}_i$, $\overline{T}_i$ and $\overline{u}_i$ are body force, surface force and displacement, respectively.

Consider the reference state of equilibrium with σ^0_{ij}, p^0_i, T^0_i and $u^0_i=0$, and then apply perturbed displacement u_i with the surface force (nodal force) increment T_i and the change of direction of body force p^0_i. The quantities appeared in Eq. (2) are then given by

$$\overline{\sigma}_{ij}=\sigma^0_{ij}+\sigma^L_{ij}+\sigma^{NL}_{ij} \qquad \overline{e}_{ij}=e^L_{ij}+e^{NL}_{ij}$$
$$\overline{p}_i=p^0_i+p^L_i \qquad \overline{T}_i=T^0_i+T_i \qquad \overline{u}_i=u_i \cdots\cdots (3\cdot a\sim e)$$

where superscript (^{0}) denotes quantity defined at the reference state, and, among the increments, (L) and (NL) indicate linear and nonlinear terms. It is noted that body force p^L_i is the linear term produced only from the change of direction. Substituting Eqs. (3) into Eq. (2) and neglecting the third and higher order terms, the virtual work equation is transformed into

$$\int_v [\sigma^0_{ij}\delta e^{NL}_{ij}+\sigma^0_{ij}\delta e^L_{ij}+\sigma^L_{ij}\delta e^L_{ij}]\,dV-\int_v [p^0_i\delta u_i+p^L_i\delta u_i]\,dV-\int_s [T^0_i\delta u_i+T_i\delta u_i]\,dS=0 \cdots\cdots (4)$$

Taking into account that the reference state satisfies the equilibrium condition in the sense of small displacements as given by

$$\int_v [\sigma^0_{ij}\delta e^L_{ij}]\,dV-\int_v [p^0_i\delta u_i]\,dV-\int_s [T^0_i\delta u_i]\,dS=0 \cdots\cdots (5)$$

Eq. (4) can be reduced to

$$\int_v [\sigma^0_{ij}\delta e^{NL}_{ij}+\sigma^L_{ij}\delta e^L_{ij}]\,dV-\int_v [p^L_i\delta u_i]\,dV-\int_s [T_i\delta u_i]\,dS=0 \cdots\cdots (6)$$

In the case of a planar straight beam element in the xz plane with x being the beam axis of centroid, Eq. (6) is written as

$$\int_v |N^0/A\delta [w'^2/2]+E[u'+zw'']\,\delta[u'+zw'']|\,dV-\int_v [p^L_i\delta u_i]\,dV-\int_s [T_i\delta u_i]\,dS=0 \cdots\cdots (7)$$

where E, A and N^0 denote Young's modulus, cross sectional area, and axial stress resultant at the

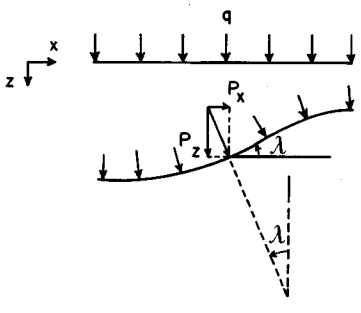

Fig. 2 Water Pressure.

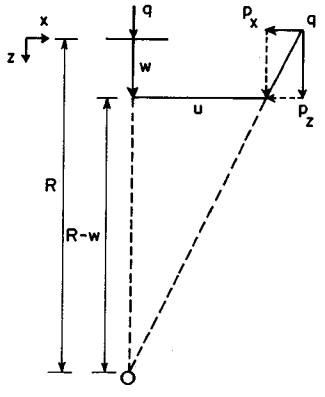

Fig. 3 Centre Directed Loading.

reference state, and ( )′ indicates differentiation with respect to x.

The second term of Eq. (7) represents the effect of the displacement dependency of loads, and then p_i^L is examined herein for the cases of water pressure and center directed loading.

The additional distributive load produced after incremental deformation from the reference state with the water pressure q can be expressed, as shown in Fig. 2, by

$$p_x=q\sin\lambda \qquad p_z=q\cos\lambda-q \cdots\cdots (8\text{-a, b})$$

Expanding the above into the Taylor series and neglecting the second and higher order terms lead to

$$p_x^L=q\lambda \qquad p_z^L=0 \cdots\cdots (9\text{-a, b})$$

As shown in Fig. 3, center directed loading produces the additional distributive force when an arbitrary point of interest experiences the incremental displacements $(u,\ w)$ as expressed by

$$p_x=-qu/h \qquad p_z=q\{R-w\}/h-q \cdots\cdots (10\text{-a, b})$$

where h is given by

$$h=[u^2+\{R-w\}^2]^{1/2} \cdots\cdots (11)$$

which is approximated by virtue of $R\gg u,\ w$ as

$$1/h=\{1+w/R\}/R \cdots\cdots (12)$$

Using Eq. (12), the linear terms of Eq. (10) is finally given as

$$p_x^L=-qu/R \qquad p_z^L=0 \cdots\cdots (13\text{-a, b})$$

It is noted that the linearization of Eqs. (9) and (13) is consistent with the present formulation to reflect the effect of the displacement dependency of loads in the virtual work equation of linearized finite displacements.

In order to derive the stiffness equation of interest, the following well-known interpolation functions of Hermite polynomials are introduced as

$$N_1=1-x/L \qquad N_2=x/L$$
$$N_3=1-3\{x/L\}^2+2\{x/L\}^3 \qquad N_4=-x+2x\{x/L\}-x\{x/L\}^2$$
$$N_5=3\{x/L\}^2-2\{x/L\}^3 \qquad N_6=x\{x/L\}-x\{x/L\}^2 \cdots\cdots (14\text{-a}\sim\text{f})$$

Using Eq. (14), displacements $(u,\ w)$ at an arbitrary point of the beam are expressed in terms of the nodal displacements $(u_i,\ w_i,\ \lambda_i,\ u_j,\ w_j,\ \lambda_j)$ as

$$u=\{A\}^t\{U\} \qquad w=\{B\}^t\{U\} \cdots\cdots (15\text{-a, b})$$

where

$$\{A\}=\{N_1\,0\,0\,N_2\,0\,0\}^t \qquad \{B\}=\{0\,N_3\,N_4\,0\,N_5\,N_6\}^t \cdots\cdots (16\text{-a, b})$$
$$\{U\}=\{u_i\ w_i\ \lambda_i\ u_j\ w_j\ \lambda_j\}^t \cdots\cdots (17)$$

Noting that the second term of Eq. (7) represents the displacement dependency of loads and the third term is the incremental nodal force, substitution of Eqs. (15) into Eq. (7) leads to the following stiffness matrix, reflecting the displacement dependency of loads, as

$$\{F\}=\{K_E+K_G+K_L\}\{U\} \cdots\cdots (18)$$

in which $\{F\}$ denotes nodal force vector, K_E and K_G are the well-known small displacement and geometrical stiffness matrices for a planar beam, as given by

$$\{F\}=\{P_{xi}P_{zi}C_i,\ P_{xj}P_{zj}C_j\}^t \cdots\cdots (19)$$

$$K_E=\int EA\{A'\}\{A'\}^t dx+\int EI\{B''\}\{B''\}^t dx \cdots\cdots (20)$$

$$K_G=\int N^0\{B'\}\{B'\}^t dx \cdots\cdots (21)$$

with I denoting the moment of inertia of beam and K_L represents the load stiffness matrix newly introduced in this study to reflect the effects of the displacement dependency of loads.

Noting the relation for Eqs. (7) and (9) as

$$p_i^L\delta u_i=q\lambda\delta u=q\{-w'\}\delta u \cdots\cdots (22)$$

the load stiffness matrix for water pressure can be expressed as

$$K_L=\int q\{A\}\{B'\}^t dx \quad (23)$$

In the case of center directed loading, noting the relation as

$$p_i^t \delta u_i=[-qu/R]\delta u \quad (24)$$

the load stiffness matrix is expressed as

$$K_L=\int q/R\{A\}\{A\}^t dx \quad (25)$$

Performing the integration for Eqs. (23) and (25), the load stiffness matrices are explicitly expressed by

$$K_L=q\begin{bmatrix} 0 & -1/2 & -L/12 & 0 & 1/2 & L/12 \\ 0 & 0 & 0 & 0 & 0 & 0 \\ 0 & 0 & 0 & 0 & 0 & 0 \\ 0 & -1/2 & L/12 & 0 & 1/2 & -L/12 \\ 0 & 0 & 0 & 0 & 0 & 0 \\ 0 & 0 & 0 & 0 & 0 & 0 \end{bmatrix} \quad (26)$$

for water pressure, and

$$K_L=q/R\begin{bmatrix} L/3 & & & & \text{Sym.} & \\ 0 & 0 & & & & \\ 0 & 0 & 0 & & & \\ L/6 & 0 & 0 & L/3 & & \\ 0 & 0 & 0 & 0 & 0 & \\ 0 & 0 & 0 & 0 & 0 & 0 \end{bmatrix} \quad (27)$$

for center directed loading.

It should be noted that the load stiffness matrix for water pressure is nonsymmetric, indicating the non-conservativeness of loading, while that for center directed loading is symmetric, making clear that the load is conservative. In case that the load is non-conservative, dynamic instability called flutter may be incurred, but it does not always happen, depending on the problems concerned. In order to examine a possibility of dynamic instability, dynamic analysis incorporating the mass matrix is required, from the nature of which it is made clear whether the dynamic instability will be involved or not through the solutions of frequency : real or complex[10].

5. BUCKLING AND FINITE DISPLACEMENT BEHAVIOR OF RINGS AND ARCHES

(1) Buckling of rings and arches

An assembly of the straight beam elements is used to approximate rings and arches for their initial geometries. The number of elements of 32 are adopted in the following computations.

Buckling of rings and arches can be investigated by performing the eigenvalue analysis for the tangent stiffness matrix including the load matrix. The internal axial stress resultant N^0 is determined by the small displacement analysis at the initial configuration subject to distributive load q. The dynamic stability analysis has been made for the case of water pressure throughout examples stated herein, and it has been confirmed that no dynamic instability occurs although the load matrix is nonsymmetric.

a) Rings

Table 1 shows the comparisons between the present FEM analysis and the existing results[3] for the buckling coefficients of rings. Since the first mode of the present analysis produces the rotation of rigid body as shown in Fig. 4 (a), resulting in trivial solutions, the buckling coefficients have been obtained for the second mode as given in Table 1 and Fig. 4 (b), and agree well with the existing results for a variety of loadings.

b) Circular arches

Buckling analysis has been performed for a hinged circular arch, as shown in Fig. 5, and the results are

Table 1 Buckling Coefficients of Ring.

		1st.Mode	2nd.Mode
COD	Ref.(3)	4.0	
	FEM	0.0	4.03
WP	Ref.(3)	3.0	
	FEM	0.0	3.02
CED	Ref.(3)	4.5	
	FEM	0.0	4.53

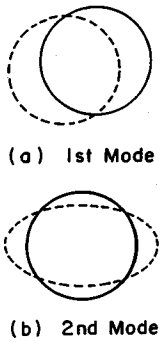

Fig. 4 Buckling Mode of Ring.

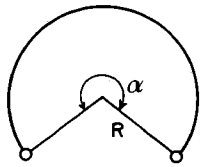

Fig. 5 A Hinged Circular Arch.

given in Table 2, indicating that the buckling coefficients do not depend so much on the loading patterns, when the subtended angle is small. However, with the increase of subtended angle, the difference becomes remarkable, reaching to the buckling coefficient for water pressure being as much as three times that for constant direction load and 5 times that for dead load, when subtended angle becomes 300 degrees, although all the values themselves are drastically decreased. A reason why the buckling coefficient becomes zero for $\alpha=360^\circ$ comes from that at this configuration the structure is a ring with one point hinged support, resulting in an unstable structure from the beginning.

Comparisons with the existing results[3] are given in Tables 3 and 4. Good agreements are observed for the constant direction loading as given in Table 3. Table 4 indicates that the existing result where its loading pattern could not be identified has agreed with the present analysis for water pressure. A similar comparison and observation of the present analysis with the existing results has been made also for the fixed circular arch, as given in Table 5 and 6.

Table 2 Buckling Coefficients of Hinged Arch.

α	60°	120°	180°	240°	300°	360°
LL	36.87	9.29	3.50	1.08	0.14	0.0
DL	35.90	8.27	2.59	0.63	0.09	0.0
COD	36.04	8.73	3.28	0.99	0.13	0.0
WP	35.09	8.00	3.01	1.25	0.44	0.0
CED	36.08	8.93	3.80	1.71	0.40	0.0

Table 3 Constant Direction Load for Hinged Arch.

α	60°	120°	180°	240°	300°	360°
Ref.(3)	36.00	8.72	3.27	1.00	0.13	0.0
COD	36.04	8.73	3.28	0.99	0.13	0.0

Table 4 Water Pressure for Hinged Arch.

α	60°	120°	180°	240°	300°	360°
Ref.(3)	35.00	8.00	3.00	1.25	0.44	0.0
WP	35.09	8.00	3.01	1.25	0.44	0.0

Table 5 Constant Direction Load for Fixed Arch.

α	60°	120°	180°	240°	300°	360°
Ref.(3)	74.94	19.59	9.00	4.63	1.99	0.70
COD	76.41	19.62	9.02	4.65	2.00	0.71

Table 6 Water Pressure for Fixed Arch.

α	60°	120°	180°	240°	300°	360°
Ref.(3)	73.32	18.14	8.00	4.59	3.27	3.00
WP	74.42	18.17	8.02	4.61	3.29	3.02

(2) Finite displacement behavior of arches

Displacement dependency of loads seems to influence not only the buckling loads but also the finite displacement post-buckling behavior of structures. In order to obtain the nonlinear behavior of arches subject to displacement dependent loading, the non-iterative analysis scheme is introduced as presented and confirmed in its precision in Refs. 10) and 11). The tangent stiffness Eq. (18) is utilized at present study, incorporating newly the external force increments in the form of the equivalent nodal force vector

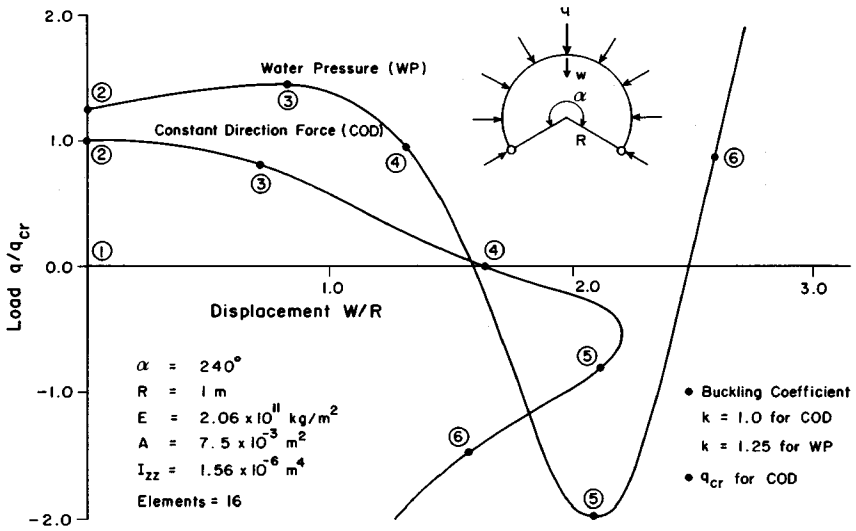

Fig. 6 Post Buckling Behavior of Circular Arch with both Ends Hinged.

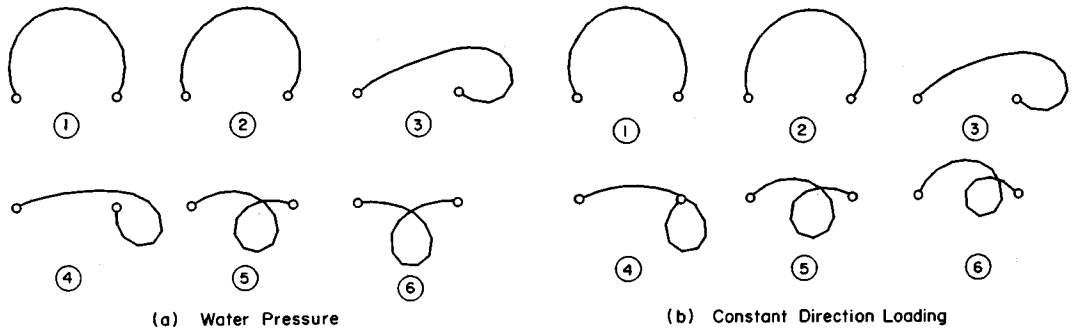

Fig. 7 Deformed Configurations of a Circular Arch with both Ends Hinged.

(see Eq. (16) in Ref. 10)) where the change of the direction of load is excluded as in the common nonlinear analysis. To avoid bifurcation in tracing the equilibrium path, a small disturbing horizontal force $P=10^{-5}$ $q_{cr}L$ is given at the crest of arch. After having confirmed that there exists no dynamic instability, the nonlinear static finite displacement analysis has been performed.

Fig. 6 shows the results of computation for a circular arch with both ends hinged. The results indicate that the displacement dependency of the load produces much more influences on the post-buckling behavior, as naturally understood by the large deformations involved. Water pressure produces the snap-through phenomenon, while the continuous unstable behavior is observed for the constant direction loading. Fig. 7 shows the deformed configurations of the hinged arch both for water pressure and the constant direction loading.

The same structure as given in the previous example but with the different boundary condition (one end fixed and the other hinged) is also investigated, and the computational results are shown in Fig. 8 for the load displacement relation, and in Fig. 9 for the deformed configurations. In this case, both of water pressure and the constant direction loading have produced the snap-through phenomena with clear distinction.

6. CONCLUDING REMARKS

Tangent stiffness equation for a planar straight beam to reflect the desplacement dependency of loadings

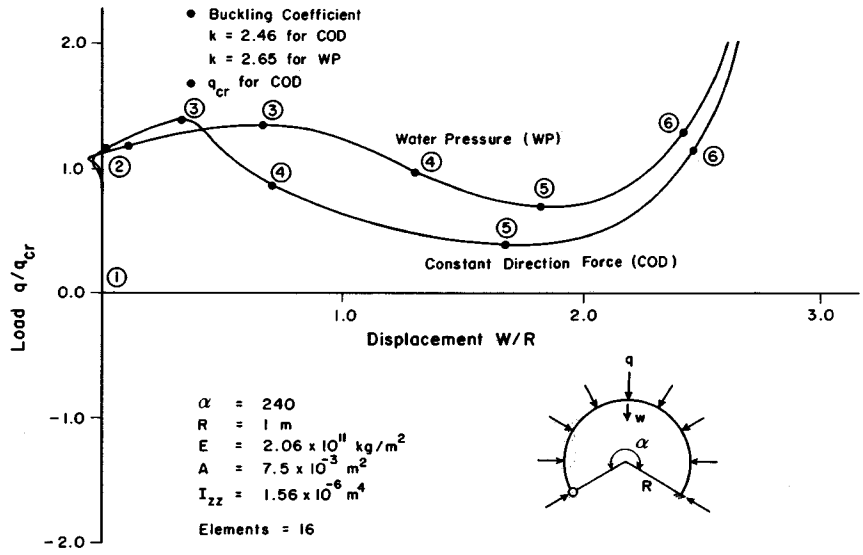

Fig. 8 Post Buckling Behavior of a Circular Arch with one End Fixed and the other Hinged.

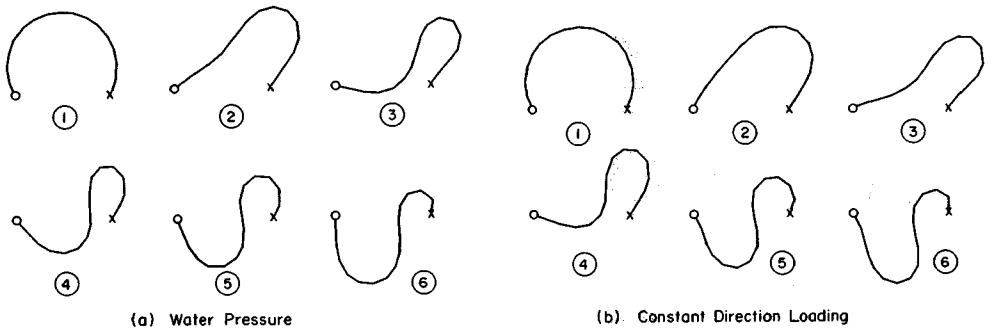

Fig. 9 Deformed Configurations of a Circular Arch with one End Fixed and the other Hinged.

has been derived, where the load stiffness matrices for water pressure and the center directed uniform distributive loading for circular members are obtained explicitly. Using the stiffness equation derived, planar buckling and post-buckling behaviors of elastic rings and arches subject to a variety of loading patterns have been examined.

The present computational results have been compared with the existing results, if available, for buckling strength. The results of buckling strength for rings have agreed well with the existing results. It has been made clear that the influences of the direction of loadings for circular arches become remarkable, when the subtended angle of arch increases. The existing results which were rather vague in their definitions have been carefully examined based on the present study.

The post-buckling nonlinear finite displacement analysis for circular arches have been successfully performed. The results indicate that the displacement dependency of loadings significantly influences the large deformation behavior of structures, more than the determination of buckling strength.

ACKNOWLEDGEMENTS : Thanks are due to Mr. Prakash Shrestha, Research Associate of the Asian Institute of Technology, for his help to finalize the preparation of manuscript.

REFERENCES

1) Bodner, S. R. : On the Conservativeness of Various Distributed Force Systems, J. Aeronout, Sci., Vol. 25, pp. 132-133, Feb.

1985.

2) Brush, D. O. and Almroth, B. O. : Buckling of Bars, Plates, Shells, McGraw-Hill, 1975.
3) C. R. C. JAPAN : Handbook of Structural Stability, Corona Publishers, Tokyo, 1971.
4) Timoshenko, S. P. and Gere, J. M. : Theory of Elastic Stability, 2nd Ed., McGraw-Hill, 1963.
5) Singer, J. and Babcock, C. D. : On the Buckling of Rings under Constant Directional and Centrally Directed Pressure, Trans. ASME, Series E, No. 1, pp. 215-218, Mar. 1970.
6) Batterman, S. C. and Soler, A. I. : Buckling of Rings, Proc. of ASCE, Vol. 96, No. EM 6, pp. 1291-1296, Dec. 1970.
7) Argysis, J. H. and Symeonidis, Sp. : Nonlinear Finite Element Analysis of Elastic Systems under Nonconservative Loading-Natural Formulation, Comp. Meths. Appl. Mech. Eng. 26, 75-123, 1981.
8) Schweizerhof, K. and Ramm, E. : Displacement Dependent Pressure Loads in Nonlinear Finite Element Analysis, Computers and Structures 18, 1984.
9) Bufler, H. : Pressure Loaded Structures under Large Deformations, Zamm. 64, 7, 287-295, 1984.
10) Hasegawa, A., Matsuno, T. and Nishino, F. : Elastic Instability and Nonlinear Analysis of Thin-Walled Members under Non-Conservative Forces, Structural Engineering/Earthquake Engineering, Vol. 5, No. 1, April 1988 (Proc. of JSCE, No. 392/ I -9).
11) Hasegawa, A., Liyanage, K. K. and Nishino, F. : A Non-Iterative Nonlinear Analysis Scheme of Space Frames with Thin-Walled Elastic Members, Structural Engineering/Earthquake Engineering, Vol. 4, No. 1, pp. 19 s-29 s, April 1987 (Proc. JSCE, No. 380/ I -7).
12) Hasegawa, A., Liyanage, K., Ikeda, T. and Nishino, F. : A Concise and Explicit Formulation of Out-of-Plane Instability of Thin-Walled Members, Structural Engineering/Earthquake Engineering, Vol. 2, No. 1, pp. 57 s-65 s, Apr. 1985 (Proc. of JSCE, No. 356/ I -3).

(Received June 6 1988)